Implementation of Roe's Method for Numerical Solution of Three-Dimensional Fluid Flow Problems with the Aid of Computer Algebra Systems

Wolfgang Schacht[1] and Evgenii V. Vorozhtsov[2]

[1] ThueringenGas, 99086 Erfurt, Stotternheimer Str. 9a, Germany; Dr_Schacht@t-online.de
[2] Institute of Theoretical and Applied Mechanics, Russian Academy of Sciences, Novosibirsk 630090, Russia; vorozh@itam.nsc.ru

Abstract. The purpose of the present paper is to extend the scope of applicability of the current computer algebra systems at the implementation of one of the popular finite difference methods for numerical solution of three-dimensional compressible fluid flow problems. This is shown at the example of an applied problem from the oil and gas industry representing the task of numerical modelling of hydrodynamic processes in spiral compensators of percussion-rotary drilling devices.

1 Introduction

At present, computer modelling of various mechanical, physical, or chemical processes contributes to the technological progress. This modelling often proves to be especially useful at the stage of a search for the optimal design solutions and reduces the price of the entire process of the development and design of new technological devices or units.

On the other hand, the development of a computer code for the modelling purpose should not take too a long time because otherwise the ready device may become antiquated by the time of its batch production. However, an attempt to speed up the process of the development of a big computer code is fraught with the introduction of numerous errors in the code.

In this connection, the attempts were undertaken repeatedly at at least partial automation of the process of the generation of PDE based computer codes. First of all, we would like to mention the following two early attempts at developing the program packages for the construction and investigation of numerical methods for solving the partial differential equations (PDEs) of the mathematical physics in the computer algebra system (CAS) environment. In [17], the REDUCE 3.3 based program package FIDE was presented. This package was designed to automate the process of numerical solving of PDE systems by means of computer algebra. This package enables the user to study both approximation and stability of finite difference schemes and to generate a FORTRAN code, which implements the chosen finite difference method.

The PDEs governing fluid flows (for example, the Navier–Stokes equations for compressible viscous fluid flow) usually contain some standard operators like the Laplacian, the gradient. One can at first derive the difference approximations to these operators and then replace with the difference operators obtained the corresponding differential operators in the system of PDEs. Such a methodology was implemented in [10] with the aid of the REDUCE system at the example of the heat equation. This idea was developed further in [18] for automatic generation of conservative scalar difference schemes for gas dynamics equations in Lagrangian form on curvilinear spatial computing meshes.

In [23], it was proposed to generate the needed FORTRAN codes for the solution of elliptic PDEs with the aid of a MACSYMA program [19].

The ideas discussed in [23] were developed significantly in [1], where the viewpoint has been expressed that the development of problem solving environments (PSEs) is needed. The final goal of a PSE is the automation of the numerical solution of initial- and boundary-value problems for PDEs, so that the PSE itself chooses a solution method for user's task. The SciNapse PSE [1] appears to be the first such PSE. This system has been implemented in *Mathematica* and produces at its output a well documented C or Fortran code.

The Ctadel system is another example of a PSE that generates efficient codes for climate models [4, 12, 20]. This is a Prolog based computer aided program implementation tool. The code generator of Ctadel was successfully applied for the generation of efficient Fortran code for the numerical weather forecast purpose.

We can identify one more direction in the solution of the problem of computer generation of executable code: the graphical object oriented modelling. This direction in the development of fast and reliable code generators is based on using the graphical description techniques like Unified Modelling Language (UML) and Object Oriented Programming (OOP) to represent the complex algorithms and data structures [11, 6–9].

There are in industrial applications many fluid mechanics problems, which are intrinsically three-dimensional. Some examples of such problems may be found in [3, 5]. A feature of these problems is that they are usually characterized by complex geometry of physical regions. By transforming a physical region to a simple region, one removes the complication of the shape of the physical region from the problems. Such transformations are carried out by introducing the curvilinear coordinate system [16]. In the present paper, we discuss the possibilities of using the computer algebra systems at various stages of the mathematical formulation and numerical solution of time dependent three-dimensional fluid flow problems in curvilinear coordinates.

The formulation of the mathematical model of flow process involves several stages:

- ❒ Derivation of analytical expressions for the metric terms in the governing PDEs in curvilinear coordinates [17, 15].
- ❒ Derivation of the formulas for boundary conditions on the curved boundaries of the physical region.
- ❒ Derivation of the equation(s) of state.

The implementation of a finite difference method for the discretization of the above formulated PDEs and boundary conditions also involves several stages:

- • Curvilinear grid generation and the check-up of grid orthogonality.
- • Derivation of the matrices of Roe's average values with regard for the chosen equation of state in the case of using the approximate Riemann solvers.
- • Specification of flux limiter functions [12].
- • Generation of Fortran or C code implementing the chosen finite-difference method [1, 4, 11, 6–9, 12, 17, 20, 23].

In the above listed stages marked with symbols ❒ and • we have also given the references to those previously published works, in which some specific stages were implemented with the aid of computer algebra systems.

The purpose of the present paper is to how how those stages, which were not implemented previously with the aid of CASs, can successfully be implemented with the aid of CASs *Mathematica* and MACSYMA. We will describe this implementation at the example of an applied problem from the oil and gas industry. This is the problem of numerical modelling of hydrodynamic processes in spiral compensators of percussion-rotary drilling devices. The percussion-rotary technique is currently the main technique for the drilling of wells in the sedimentary rocks for the exploratory purposes and oil and natural gas production. This technique is inefficient at the drilling in hard crystalline rocks [21, 29]. The percussion-rotary drilling is a combination of the rotary and percussion methods and has the following advantages over the pure rotary drilling:

- – higher drilling velocity in moderately hard and hard stone;
- – better stability of well direction and
- – insignificant wear because of lesser rotation frequency and lesser drilling pressure.

The numerical modelling of hydraulic shocks inside the work volume of a percussion-rotary drilling hammer (PRDH) was carried out previously with the aid of the method of characteristics in one-dimensional formulation; a review of relevant works as well as the numerical algorithm taking into account the possibility of cavities formation may be found in [29]. A detailed description of the hydrodynamic processes occurring in the PRDH work volume within a single work cycle has been

presented in [22]. During this cycle, two shock waves arise: the first of them, the strongest one, impinges onto the piston, which hits the anvil of the hammer, and the second shock propagates upwards through the spiral compensator in the direction opposite to the motion of the working liquid, the distilled water, which is pumped into the hammer.

A further increase in the PRDH efficiency is related to an increase in the strength of the shock wave impinging onto the anvil. But this also leads to an increase in the strength of a shock wave propagating upwards in the spiral compensator. The main task of this compensator is to maximally damp the shock for the purpose of avoiding the rupture of the entire PRDH device. Thus, a search for the ways of optimization of the design of spiral compensators is a challenging problem for the design of the new PRDHs. The numerical modelling is here a very efficient means because the manufacturing of the full-scale test samples of new compensators requires considerable expenses in connection with high requirements for compensator strength.

In the one-dimensional formulation the numerical modelling of time dependent hydrodynamic processes in spiral compensators was implemented for the first time in the work [22]. The following two second-order difference schemes were used therein: a scheme of the "cross" type and a TVD scheme adapted to the barotropic fluid flows. As a result, the optimal configurations of spiral compensators were found in [22], which ensure the best damping effect under the existing technological constraints for the PRDH dimensions.

The mathematical model of one-dimensional flow does, however, not take into account the effect of the curvature of the spiral channel walls as well as the possible effects of the shock reflection from the walls. Therefore, a modelling on the basis of a model of three-dimensional flow of an inviscid compressible barotropic fluid with regard for friction forces is a more complete mathematical modelling of shock wave processes in spiral compensators.

We briefly describe in the following both the mathematical model of the 3D fluid flow in the spiral compensator channel and the numerical method for the discretization of the equations of this model and show how the above listed stages of the mathematical modelling of a complex applied problem under consideration were implemented with the aid of CASs *Mathematica* and MACSYMA.

2 Governing Equations

The equations governing a three-dimensional nonstationary flow of an inviscid compressible non-heat-conducting barotropic fluid in the rectangular Cartesian coordinates x, y, z have the following form [26]

$$\frac{\partial \rho}{\partial t} + \nabla \cdot (\rho \boldsymbol{v}) = 0, \tag{1}$$

$$\frac{\partial \left(\rho \vec{v}\right)}{\partial t} + \nabla \cdot (\rho \boldsymbol{v}\boldsymbol{v}) + \nabla p = \rho \boldsymbol{g} - \rho \frac{\lambda}{2D} |\boldsymbol{v}| \cdot \boldsymbol{v}. \tag{2}$$

Equations (1) and (2) represent the differential forms of writing the conservation laws for the mass and momentum. In Eqs. (1), (2) ρ is the fluid density; $\boldsymbol{v} = (u, v, w)$ is the vector of fluid velocity, where u, v, w are the components of the velocity vector along the x-, y-, and z-axis, respectively; p is the pressure, and $\boldsymbol{g}$ is the vector of acceleration due to gravity (9.81 m/s^2) and $|\boldsymbol{v}|$ is the modulus of the velocity vector, that is $|\boldsymbol{v}| = \sqrt{u^2 + v^2 + w^2}$. The term $-\rho\lambda|\boldsymbol{v}| \cdot \boldsymbol{v}/(2D)$ in equation (2) takes into account the losses due to wall friction in channel. We have used in the present work the following relations basing on the experimental data:

$$D = \frac{B_1 H_1}{B_1 + H_1}, \qquad \lambda = \frac{0.021}{D^{0.3}} \tag{3}$$

for the computation of the effective diameter D and the wall friction number λ [22]. Here B_1 and H_1 are the internal dimensions of flow channel (see Fig. 1) in a cross section, which is perpendicular to the channel walls. The componentwise form of equations (1) and (2) is as follows:

$$\frac{\partial \mathbf{U}}{\partial t} + \frac{\partial \mathbf{F}(\mathbf{U})}{\partial x} + \frac{\partial \mathbf{G}(\mathbf{U})}{\partial y} + \frac{\partial \mathbf{H}(\mathbf{U})}{\partial z} = \mathbf{R}(\mathbf{U}), \tag{4}$$

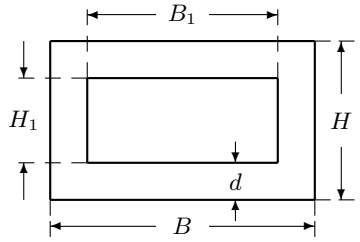

Fig. 1. The rectangular cross section of a spiral channel.

where

$$\mathbf{U} = \begin{pmatrix} \rho \\ \rho u \\ \rho v \\ \rho w \end{pmatrix},\ \mathbf{F}(\mathbf{U}) = \begin{pmatrix} \rho u \\ \rho u^2 + p \\ \rho uv \\ \rho uw \end{pmatrix},\ \mathbf{G}(\mathbf{U}) = \begin{pmatrix} \rho v \\ \rho uv \\ \rho v^2 + p \\ \rho vw \end{pmatrix},\ \mathbf{H}(\mathbf{U}) = \begin{pmatrix} \rho w \\ \rho uw \\ \rho vw \\ \rho w^2 + p \end{pmatrix},$$

$$\mathbf{R}(\mathbf{U}) = \begin{pmatrix} 0 \\ -\lambda\rho|\boldsymbol{v}|u/(2D) \\ -\lambda\rho|\boldsymbol{v}|v/(2D) \\ -\lambda\rho|\boldsymbol{v}|w/(2D) - \rho g \end{pmatrix}. \tag{5}$$

Since the spiral channel walls are curved it is more convenient to use the equations of fluid flow in curvilinear coordinates ξ, η, ζ such that the original region Ω in the space of the Cartesian coordinates x, y and z is mapped onto a parallelogram Π in the space of curvilinear coordinates. Assume that there is the corresponding one-to-one mapping

$$x = x(\xi, \eta, \zeta), \quad y = y(\xi, \eta, \zeta), \quad z = z(\xi, \eta, \zeta), \quad (\xi, \eta, \zeta) \in \Pi. \tag{6}$$

The flow equations (1)–(2) in curvilinear coordinates ξ,η, and ζ take the following form (Pulliam and Steger 1980, Vatsa 1987, Vatsa and Wedan 1988):

$$\frac{\partial \mathbf{U}J}{\partial t} + \frac{\partial \hat{\mathbf{F}}}{\partial \xi} + \frac{\partial \hat{\mathbf{G}}}{\partial \eta} + \frac{\partial \hat{\mathbf{H}}}{\partial \zeta} = J\mathbf{R}(\mathbf{U}). \tag{7}$$

Here J is the Jacobian of transformation (6),

$$J = x_\xi(y_\eta z_\zeta - y_\zeta z_\eta) - y_\xi(x_\eta z_\zeta - x_\zeta z_\eta) + z_\xi(x_\eta y_\zeta - y_\eta x_\zeta). \tag{8}$$

$x_\xi, y_\xi, z_\xi, x_\eta, y_\eta, z_\eta, x_\zeta, y_\zeta, z_\zeta$ are the partial derivatives, for example, $z_\eta = \partial z(\xi,\ \eta,\ \zeta)/\partial\eta$, etc.;

$$\hat{\mathbf{F}} = J\xi_x\mathbf{F} + J\xi_y\mathbf{G} + J\xi_z\mathbf{H},\ \hat{\mathbf{G}} = J\eta_x\mathbf{F} + J\eta_y\mathbf{G} + J\eta_z\mathbf{H},\ \hat{\mathbf{H}} = J\zeta_x\mathbf{F} + J\zeta_y\mathbf{G} + J\zeta_z\mathbf{H}, \tag{9}$$

where the column vectors **F, G**, and **H** are defined by formulas (5).

The metric terms $\xi_x, \xi_y, \ldots, \zeta_z$ entering (9) may be expressed in terms of the derivatives $x_\xi, x_\eta, \ldots, z_\zeta$ via the formulas (Pulliam and Steger 1980)

$$\begin{aligned} \xi_x &= (y_\eta z_\zeta - y_\zeta z_\eta)/J, \quad \xi_y = (z_\eta x_\zeta - x_\eta z_\zeta)/J, \quad \xi_z = (x_\eta y_\zeta - y_\eta x_\zeta)/J, \\ \eta_x &= (z_\xi y_\zeta - y_\xi z_\zeta)/J, \quad \eta_y = (x_\xi z_\zeta - x_\zeta z_\xi)/J, \quad \eta_z = (y_\xi x_\zeta - x_\xi y_\zeta)/J, \\ \zeta_x &= (y_\xi z_\eta - z_\xi y_\eta)/J, \quad \zeta_y = (x_\eta z_\xi - x_\xi z_\eta)/J, \quad \zeta_z = (x_\xi y_\eta - y_\xi x_\eta)/J. \end{aligned} \tag{10}$$

The Jacobian J must be different from zero at $(\xi, \eta, \zeta) \in \Pi$ to ensure the singlevaluedness of transformation (6).

Applying the methods of analytic geometry it is not difficult to show that the desired mapping (9) has the following form for the case of a spiral channel:

$$x = \Big(B_1\eta + a - \frac{B_1}{2}\Big)\cos\xi,\ y = -\Big(B_1\eta + a - \frac{B_1}{2}\Big)\sin\xi,\ z = \bar{H}_1\zeta + c_1\xi - \frac{\bar{H}_1}{2},$$
$$s_{\min} \le \xi \le s_{\max}, \quad 0 \le \eta \le 1, \quad 0 \le \zeta \le 1. \tag{11}$$

The quantity $\bar{H}_1$ entering (11) is related to the vertical size H_1 of the hydraulic cross section by formula $\bar{H}_1 = H_1/\sin\alpha$, where α is the angle between the tangent to the spiral midline of the channel and the positive direction of the Oz-axis, $0 < \alpha < \pi/2$.

Owing to the availability of analytic expressions (11) for the functions $x(\xi,\eta,\zeta)$, $y(\xi,\eta,\zeta)$, $z(\xi,\eta,\zeta)$ we can obtain the analytic expressions for all metric derivatives ξ_x, ξ_y,...,ζ_z entering the expressions for the fluxes (9). These metric derivatives were obtained with the aid of symbolic computations on a desktop computer with the use of the software package *Mathematica 4.1*. In particular, the metric derivatives x_ξ and x_η were computed with *Mathematica* as follows:

```
x[u_,v_,w_] := (a + B1*v-B1/2)*Cos[u];
xksi = D[x[u,v,w],u]; xeta = D[x[u,v,w], v];

Rule1 = {u→ ξ, v→ η, w→ ζ, B1→ B1, H1→ H1, c1→ c1};
{xksi1, xeta1} = {xksi, xeta}/.Rule1;
Print["xξ= ", TraditionalForm[xksi1], "; xη= ", TraditionalForm[xeta1]];
```

$$x_\xi = -\sin(\xi)\Big(a + \eta B_1 - \frac{B_1}{2}\Big); \quad x_\eta = \cos(\xi)B_1$$

The Jacobian J was then computed symbolically with *Mathematica* by substituting the found expressions for the metric derivatives into formula (8) and was found to have the following form:

$$J = B_1\bar{H}_1[a + B_1(\eta - 0.5)]. \tag{12}$$

The factor $a + B_1(\eta - 0.5)$ satisfies the inequalities:

$$a - 0.5B_1 \le a + B_1(\eta - 0.5) \le a + 0.5B_1. \tag{13}$$

By virtue of the inequalities $a > B/2 > B_1/2$ it follows from (13) that always $J > 0$. Thus, the transformation (6), (11) is always single-valued.

3 Equation of State

To close the system of the Euler equations (1), (2) it is desirable to use a fluid equation of state, which takes into account a rectangular cross section of the pipe and the elastic deformations of the metal pipe walls when a shock wave passes periodically through the liquid in the pipe. Such an equation of state was derived by Jenkner [14, 24]. Prior to using this equation of state in our computations we have decided to check the Jenkner's derivations. For this purpose we have used the CAS MACSYMA [19].

For the pressure wave velocity a in any pipe cross section the following relation holds [13]:

Eq_1_1: a=sqrt((1/rho)/((1/rho)*diff(rho,p)+ (1/\a)*diff(\a(p),p)))

$$\mathrm{a} = \sqrt{\frac{1}{\rho\left(\frac{\frac{d}{dp}(A(p))}{A} + \frac{\frac{d\rho}{dp}}{\rho}\right)}}$$

where $A(p)$ is the pipe cross section area, ρ is the fluid density. For an infinitely rigid pipe wall $dA(p)/dp = 0$, and in this case the sound velocity in any cross section of the pipe coincides with the sound velocity in fluid:

Eq_1_1_1: subst(0, a(p), Eq_1_1)

$$\mathrm{a} = \sqrt{\frac{1}{\frac{d\rho}{dp}}}$$

If one takes into account the elasticity of pipe walls then one can assume with regard for the classical elasticity theory that the volume contraction of the fluid element $(1/\rho)(d\rho/dp)$ may be replaced with the aid of formula

$$(1\rho)(d\rho/dp) = 1/K, \tag{14}$$

where K is the fluid bulk modulus. We can then write the formula for sound velocity as Eq_1_2:

ratsubst(1/\k,(1/rho)*diff(rho,p),Eq_1_1_1)

$$\mathrm{a} = \sqrt{\frac{K}{\rho}}$$

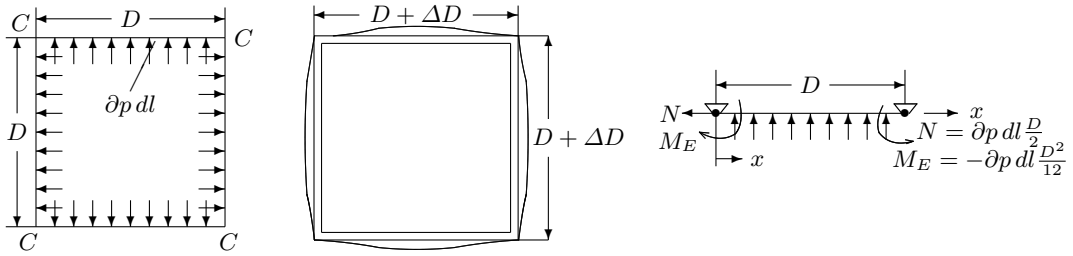

(a) (b) (c)

Fig. 2. The loading on a pipe with square cross section and its deformation: (a) the loading; (b) the cross section deformation; (c) the bar clamped at its ends.

A relative distension of the pipe cross section $(1/A)(dA(p)/dp)$ takes various values depending on a specific geometric shape of the pipe cross section. We consider the case when the cross section is a square with the side length D. Let us take a pipe element of length dl and let δp be the internal fluid pressure. Due to the axial and diagonal symmetry the distance between the neighboring points C (Fig. 1, a) will be the same and equal to $D + \delta D$. The deformation pattern of a square frame under the internal pressure is obtained as shown in Fig. 1, b. The total increase dA in the area is composed as a sum of the distension δA_N due to normal forces N and the flexional distension δA_B. The area increment can then be computed as a consequence of the distension of a bar clamped at its ends, but extensible in the direction along the bar, see Fig. 1, c.
The distension due to normal forces:

simp: false $
Eq1_3_1: \delta*\d=sigma[\n]*\d/\e

$$\Delta D = \frac{\sigma_N}{E}$$

Here E is the Young's module of the wall material, σ_N is the normal stress. With $N = dp\,dl\,D/2$ and $\sigma_N = N/(e\,dl) = dp\,D/(2e)$, where e is the wall thickness, we have:

simp: false $
Eq1_3_2: \delta*\d=dp*\d^2/(2*e*\e)

$$\Delta D = \frac{dp\,D^2}{2eE}$$

The total area increase for the entire frame is obviously

Eq1_4_1: delta*\a[\n]=4*((\d*\delta*\d/2+(\delta*\d^2/4))

$$\delta A_N = 4\left(\frac{D\,\Delta D}{2} + \frac{(\Delta D)^2}{4}\right)$$

Neglecting the small term of the order $(\Delta D)^2$ we obtain:

Eq1_4_2: delta*\a[\n]=2*\d*\delta*\d

$$\delta A_N = 2D\,\Delta D$$

or with regard for equation Eq_1_3_2

Eq1_4_3: delta*\a[\n]=dp*\d^3/(e\e)

$$\delta A_N = \frac{dp\, D^3}{eE}.$$

The area distension δA_B is found as an area between the straight axis and the flexion line of the bar clamped at its both ends under a continuous loading $\delta p\, \delta l$. The flexion line has the form [14]

Eq1_4_4: y=(dp*dl*\d^4/(24*\e*\j))*((x/\d)- 2*(x^3/(\d^3))+(x^4/(\d^4)))

$$y = \frac{dp\ dl\ D^4 \left(\frac{x}{D} - \frac{2x^3}{D^3} + \frac{x^4}{D^4}\right)}{24E\, J},$$

where J is the inertia moment. After the integration we obtain for the bar:

simp: true$
Eq1_4_5: delta*\a[\b,1]= 'integrate(rhs(Eq_1_4_4),x,0,\d)

$$\delta A_{B,1} = \frac{dl\ dp \left(\int_0^D \left(\frac{x}{D} - \frac{2x^3}{D^3} + \frac{x^4}{D^4}\right) dx\right) D^4}{24E\, J}.$$

Eq1_4_6: Eq_1_4_5, integrate

$$\delta A_{B,1} = \frac{dl\, dp\, D^5}{120E\, J}.$$

Jenkner [14] had obtained the factor 720 in the denominator of the formula for $\delta A_{B,1}$. With

Eq1_4_7: \j=dl*e^3/12

$$J = \frac{dl\, e^3}{12}$$

this implies

Eq1_5_1: subst(rhs(Eq_1_4_7),\j,Eq_1_4_6)

$$\delta A_{B,1} = \frac{dp\, D^5}{10e^3 E}.$$

A comparison of δA_N and δA_B yields

Eq1_6_1: rhs(Eq_1_6_1)/rhs(Eq_1_4_3)

$$\frac{D^2}{10e^2}$$

This means that the area increment due to flexional distension is much predominant, so that for pipes with $D/e > 20$ one can neglect the contribution of δA_N to the total area distension. From Eq_1_5_1 and the area $A = D^2$ one can find the relative area distension:

Eq1_7_1: (1/\a)*'diff(\a(p),p)= \d^3/(10*e^3*\e)

$$\frac{\frac{d}{dp}(A(p))}{A} = \frac{D^3}{10e^3 E}.$$

This results in the following formula for sound velocity in a pipe with square cross section:

Eq1_8_1: subst(\d^3/(10*e^3 * \e), (1/\a)*diff(\a(p),p),Eq_1_1)

$$\mathrm{a} = \sqrt{\frac{1}{\rho\left(\frac{D^3}{10e^3 E} + \frac{\frac{d\rho}{dp}}{\rho}\right)}}.$$

Eq1_8_2: subst((1/\k),(1/rho)*diff(rho,p),Eq_1_8_1)

$$\mathrm{a} = \sqrt{\frac{1}{\rho\left(\frac{1}{K} + \frac{D^3}{10e^3 E}\right)}}\ .$$

Since $dp/d\rho = \mathrm{a}^2$, the integration

$$p = \int_{\rho_0}^{\rho} \mathrm{a}^2 d\rho$$

obviously yields the following formula for the equation of state in the case of a square cross section, where ρ_0 is the initial fluid density at $t = 0$:

$$p = \left(\frac{1}{\frac{1}{K} + \frac{D^3}{10e^3 E}} \right) \ln \frac{\rho}{\rho_0} \ .$$

Jenkner [14] has extended the above derivation for the case of a rectangular cross section, and the final equation of state, with regard for our correction found above with the aid of CAS MACSYMA, has the form

$$p = K_{\text{eff}} \cdot \ln(\rho/\rho_0) \tag{15}$$

with

$$K_{\text{eff}} = \left(\frac{1}{E_F} + \frac{(B/H)^4 R(\beta)}{10(d/H)^3 E_M} \right)^{-1} , \tag{16}$$

where E_F and E_M are the Young's modules of elasticity for fluid and wall material, respectively, d is the wall thickness, and B or H are the external dimensions of the channel cross section (see Fig. 1). The quantity $R(\beta)$ is the so-called rectangular factor:

$$R(\beta) = \frac{1}{2}(6 - 5\beta) + \frac{1}{2} \left(\frac{H}{B} \right)^5 \left(6 - 5\beta \left(\frac{B}{H} \right)^2 \right), \quad \beta = 1 - \frac{H}{B} + \left(\frac{H}{B} \right)^2 . \tag{17}$$

Note that Jenkner [14] has derived the factor K_{eff} by hand in the form

$$K_{\text{eff}} = \left(\frac{1}{E_F} + \frac{(B/H)^4 R(\beta)}{15(d/H)^3 E_M} \right)^{-1} .$$

We have used the equation of state (15) with formula (16) for K_{eff} in our three-dimensional computations of fluid flow in a spiral channel.

4 Boundary Conditions

We now show the efficiency of using the CAS *Mathematica* while obtaining the analytic expressions for the boundary conditions on the spiral channel walls in curvilinear coordinates. We will consider for the purpose of brevity only the case of the lower channel wall. The value $\zeta = 0$ of the curvilinear coordinate ζ in (11) corresponds to this wall. Thus, the parametric equations of the lower wall are as follows:

$$x = \left(B_1 \eta + a - \frac{B_1}{2} \right) \cos\xi, \ y = -\left(B_1 \eta + a - \frac{B_1}{2} \right) \sin\xi, \ z = c_1 \xi - \frac{\bar{H}_1}{2}, \tag{18}$$
$$s_{\min} \le \xi \le s_{\max}, \ 0 \le \eta \le 1.$$

Let us find the form of the boundary condition $v_n = 0$ on the lower channel wall. We make use of the formula $v_n = \boldsymbol{v} \cdot \boldsymbol{n}$, where $\boldsymbol{n}$ is the unit normal vector to the lower wall. According to (18) the equations for the lower wall have the form: $x = x(\xi, \eta)$, $y = y(\xi, \eta)$, $z = z(\xi)$. The unit normal to the surface (18) is computed by formula [2]

$$\boldsymbol{n} = \frac{\frac{\partial(y,z)}{\partial(\xi,\eta)} \boldsymbol{i} + \frac{\partial(z,x)}{\partial(\xi,\eta)} \boldsymbol{j} + \frac{\partial(x,y)}{\partial(\xi,\eta)} \boldsymbol{k}}{\sqrt{\left[\frac{\partial(y,z)}{\partial(\xi,\eta)} \right]^2 + \left[\frac{\partial(z,x)}{\partial(\xi,\eta)} \right]^2 + \left[\frac{\partial(x,y)}{\partial(\xi,\eta)} \right]^2}},$$

where

$$\frac{\partial(y,z)}{\partial(\xi,\eta)} = \begin{vmatrix} \frac{\partial y}{\partial \xi} & \frac{\partial z}{\partial \xi} \\ \frac{\partial y}{\partial \eta} & \frac{\partial z}{\partial \eta} \end{vmatrix}, \quad \frac{\partial(z,x)}{\partial(\xi,\eta)} = \begin{vmatrix} \frac{\partial z}{\partial \xi} & \frac{\partial x}{\partial \xi} \\ \frac{\partial z}{\partial \eta} & \frac{\partial x}{\partial \eta} \end{vmatrix}, \quad \frac{\partial(x,y)}{\partial(\xi,\eta)} = \begin{vmatrix} \frac{\partial x}{\partial \xi} & \frac{\partial y}{\partial \xi} \\ \frac{\partial x}{\partial \eta} & \frac{\partial y}{\partial \eta} \end{vmatrix}. \tag{19}$$

All determinants in (19) were computed symbolically. In particular, the determinant $\partial(y,z)/\partial(\xi,\eta)$ was computed with the aid of *Mathematica* as follows:

```
TraditionalForm[Det[{{D[y[u,v,w], u], D[z[u,v,w], u]}, {D[y[u,v,w],v],
D[z[u,v,w], v]}}]/.Rule1]
```

$$sin(\xi)B_1c_1$$

Thus,

$$\frac{\partial(y,z)}{\partial(\xi,\eta)} = B_1c_1\sin\xi, \quad \frac{\partial(z,x)}{\partial(\xi,\eta)} = B_1c_1\cos\xi, \quad \frac{\partial(x,y)}{\partial(\xi,\eta)} = B_1[a + B_1(\eta - 0.5)];$$

$$\sqrt{\left[\frac{\partial(y,z)}{\partial(\xi,\eta)}\right]^2 + \left[\frac{\partial(z,x)}{\partial(\xi,\eta)}\right]^2 + \left[\frac{\partial(x,y)}{\partial(\xi,\eta)}\right]^2} = \frac{1}{2}B_1\sqrt{(B_1 - 2a - 2B_1\eta)^2 + 4c_1^2}.$$

From the condition $v_n = 0$ on the lower wall we obtain the equation:

$$uc_1\sin\xi + vc_1\cos\xi + w[a + B_1(\eta - 0.5)] = 0.$$

The boundary condition $\partial p/\partial n = 0$ on the lower wall is derived with the aid of the formula $\partial p/\partial n = \nabla p \cdot \boldsymbol{n}$ and leads to the following equality:

$$\frac{\partial p}{\partial x}c_1\sin\xi + \frac{\partial p}{\partial y}c_1\cos\xi + \frac{\partial p}{\partial z}\cdot[a + B_1(\eta - 0.5)] = 0.$$

5 The Roe's Method

The Roe's method has gained a widespread acceptance as an efficient method for the solution of fluid dynamics problems [25]. It was implemented by us on a curvilinear spatial curvilinear grid of quadrilateral cells. Using the analytic formulas (**??**) it is easy to generate numerically this grid. For this purpose we at first construct an uniform grid in the parallelepiped Π defined as the region $\Pi = \{(\xi,\eta,\zeta)|\ s_{\min} \le \xi \le s_{\max}, \quad 0 \le \eta \le 1, \quad 0 \le \zeta \le 1\}$. Let

$$\xi_i = s_{\min} + (i-1)\Delta\xi,\ i = 1,\ldots,N_1;\ \eta_j = (j-1)\Delta\eta,\ j = 1,\ldots,N_2;\ \zeta_k = (k-1)\Delta\zeta,\ k = 1,\ldots,N_3,$$

where $N_1 > 1$, $N_2 > 1$, and $N_3 > 1$ are the user-specified numbers of the grid nodes in the directions of the axes ξ, η, ζ, respectively; $\Delta\xi$, $\Delta\eta$, $\Delta\zeta$ are the uniform grid steps along the axes ξ, η, ζ, respectively; $\Delta\xi = (s_{\max} - s_{\min})/(N_1 - 1)$, $\Delta\eta = 1/(N_2 - 1)$, $\Delta\zeta = 1/(N_3 - 1)$. An arbitrary grid node in Π is the point with coordinates $(\xi_i,\ \eta_j,\ \zeta_k)$. In the space of the physical coordinates $(x,\ y,\ z)$ the node $(x_{ijk}, y_{ijk}, z_{ijk})$ corresponds to this point, where

$$x_{ijk} = \left(B_1\eta_j + a - \frac{B_1}{2}\right)\cos\xi_i\ ,\ y_{ijk} = -\left(B_1\eta_j + a - \frac{B_1}{2}\right)\sin\xi_i\ ,\ z_{ijk} = \bar{H}_1\zeta_k + c_1\xi_i - \frac{\bar{H}_1}{2}. \quad (20)$$

It is easy to show that the generated curvilinear grid is orthogonal. The conditions for the orthogonality of different families of grid lines to one another may indeed be written as $x_\xi x_\eta + y_\xi y_\eta + z_\xi z_\eta = 0$, $x_\xi x_\zeta + y_\xi y_\zeta + z_\xi z_\zeta = 0$, $x_\eta x_\zeta + y_\eta y_\zeta + z_\eta z_\zeta = 0$. We have checked these conditions with *Mathematica* by substituting into them the relations for the metric derivatives, which were also computed with *Mathematica* as this was demonstrated above. We have found in this way that all the orthogonality relations are satisfied.

Fig. 3 gives an idea of the curvilinear grid computed by formulas (20). It can be seen from this figure that the presented spiral compensator has 12 rolls, so that the total angle of the turn of the the vector tangent to the external vertical wall amounts to $360^\circ \cdot 12 = 4320^\circ$. Note that the largest angle of the tangent vector turn, which we have found in the literature, amounts to only 540° in the two-dimensional computations reported in [27].

Since the number of rolls in Fig. 3 is 12, about 13 grid nodes along the ξ-axis lie within each single roll. The obtained grid on the internal surface may be seen to be insufficiently smooth, so that it is desirable to take a larger number than 161 of nodes along the ξ-axis for the given compensator.

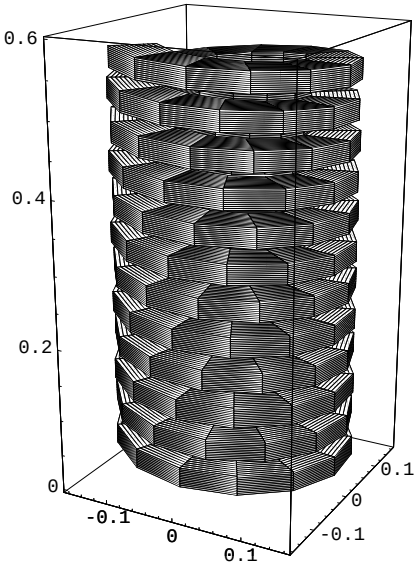

Fig. 3. The curvilinear grid on the internal walls of a spiral channel for $N_1 = 161$, $N_2 = 12$, $N_3 = 12$. The dimensions are given in meters.

At the extension of the Roe's scheme for the three-dimensional case we will need the expansions:

$$\hat{\mathbf{A}} = \mathbf{R}_1 \mathbf{\Lambda}_1 \mathbf{R}_1^{-1}; \quad \hat{\mathbf{B}} = \mathbf{R}_2 \mathbf{\Lambda}_2 \mathbf{R}_2^{-1}; \quad \hat{\mathbf{C}} = \mathbf{R}_3 \mathbf{\Lambda}_3 \mathbf{R}_3^{-1}, \tag{21}$$

where $\mathbf{\Lambda}_1$, $\mathbf{\Lambda}_2$, and $\mathbf{\Lambda}_3$ are the diagonal matrices whose principal diagonals are occupied by the eigenvalues of matrices $\hat{\mathbf{A}}$, $\hat{\mathbf{B}}$, and $\hat{\mathbf{C}}$, respectively; $\mathbf{R}_1$, $\mathbf{R}_2$, and $\mathbf{R}_3$ are certain nonsingular matrices.

We will assume that the components of the vector $\mathbf{U}_{ijk}^n$ are computed at the cell center in the space of the (ξ, η, ζ), that is at point with the coordinates ($\xi_{i+1/2}$, $\eta_{j+1/2}$, $\zeta_{k+1/2}$), where

$$\xi_{i+1/2} = s_{\min} + (i - 0.5)\Delta\xi, \; i = 1, \ldots, N_1; \quad \eta_{j+1/2} = (j - 0.5)\Delta\eta, \; j = 1, \ldots, N_2 - 1;$$
$$\zeta_{k+1/2} = (k - 0.5)\Delta\zeta, \; k = 1, \ldots, N_3 - 1.$$

The Roe's scheme as applied to system (7) may be written as

$$\frac{\left(\mathbf{U}_{ijk}^{n+1} - \mathbf{U}_{ijk}^n\right) J_{ijk}}{\tau} + \frac{\mathbf{\Phi}_{i+1/2,j,k}^n - \mathbf{\Phi}_{i-1/2,j,k}^n}{\Delta\xi} + \frac{\mathbf{\Psi}_{i,j+1/2,k}^n - \mathbf{\Psi}_{i,j-1/2,k}^n}{\Delta\eta}$$
$$+ \frac{\mathbf{\Gamma}_{i,j,k+1/2}^n - \mathbf{\Gamma}_{i,j,k-1/2}^n}{\Delta\zeta} = J_{ijk} \mathbf{R}_{ijk}^n, \tag{22}$$

where the fluxes $\Phi_{i\pm1/2,j,k}^n$, $\Psi_{i,j\pm1/2,k}^n$, $\Gamma_{i,j,k\pm1/2}^n$ are computed by formulas:

$$\mathbf{\Phi}_{i+1/2,j,k}^n = \frac{1}{2}\left[\hat{\mathbf{F}}\left(\mathbf{U}_{ijk}^n\right) + \hat{\mathbf{F}}\left(\mathbf{U}_{i+1,j,k}^n\right)\right] - \frac{1}{2}\left(\mathbf{R}_1 \psi\left(\mathbf{\Lambda}_1\right) \mathbf{R}_1^{-1}\right)\left(\bar{\mathbf{U}}_{i+1/2}\right)\left(\mathbf{U}_{i+1,j,k}^n - \mathbf{U}_{ijk}^n\right), \tag{23}$$

$$\mathbf{\Psi}_{i,j+1/2,k}^n = \frac{1}{2}\left[\hat{\mathbf{G}}\left(\mathbf{U}_{ijk}^n\right) + \hat{\mathbf{G}}\left(\mathbf{U}_{i,j+1,k}^n\right)\right] - \frac{1}{2}\left(\mathbf{R}_2 \psi\left(\mathbf{\Lambda}_2\right) \mathbf{R}_2^{-1}\right)\left(\bar{\mathbf{U}}_{j+1/2}\right)\left(\mathbf{U}_{i,j+1,k}^n - \mathbf{U}_{ijk}^n\right), \tag{24}$$

$$\mathbf{\Gamma}_{i,j,k+1/2}^n = \frac{1}{2}\left[\hat{\mathbf{H}}\left(\mathbf{U}_{ijk}^n\right) + \hat{\mathbf{H}}\left(\mathbf{U}_{i,j,k+1}^n\right)\right] - \frac{1}{2}\left(\mathbf{R}_3 \psi\left(\mathbf{\Lambda}_3\right) \mathbf{R}_3^{-1}\right)\left(\bar{\mathbf{U}}_{k+1/2}\right)\left(\mathbf{U}_{i,j,k+1}^n - \mathbf{U}_{ijk}^n\right). \tag{25}$$

In (23) — (25)

$$\psi(\mathbf{\Lambda}_m) = \mathrm{diag}\left(\psi\left(\lambda_1^{(m)}\right), \psi\left(\lambda_2^{(m)}\right), \psi\left(\lambda_3^{(m)}\right), \psi\left(\lambda_4^{(m)}\right)\right), \quad m = 1, 2, 3. \tag{26}$$

and

$$\psi(z) = \begin{cases} |z|, & |z| \geq \delta \\ \frac{z^2 + \delta^2}{2\delta}, & |z| < \delta \end{cases}, \tag{27}$$

δ is a user-specified positive constant. At $z = 0$ we obtain from (27): $\psi(0) = 0.5\delta$. Thus, owing to the introduction of the function (27) the dissipativity of the difference scheme is ensured also in those flow subregions, where some of the eigenvalues $\lambda_\mu^{(m)}$ change their signs.

The quantities $\bar{\mathbf{U}}_{i+1/2}$, $\bar{\mathbf{U}}_{j+1/2}$, and $\bar{\mathbf{U}}_{k+1/2}$ in formulas (23), (24), and (25), respectively, are the Roe's averages. The Roe averages representing the components of the vector $\bar{\mathbf{U}}_{i+1/2}$ entering equations (23) have the following form for the case of the equation of state (15):

$$\bar{u}_{i+1/2} = \frac{\sqrt{\rho_{ijk}}u_{ijk}+\sqrt{\rho_{i+1,j,k}}u_{i+1,j,k}}{\sqrt{\rho_{ijk}}+\sqrt{\rho_{i+1,j,k}}}\,; \quad \bar{v}_{i+1/2} = \frac{\sqrt{\rho_{ijk}}v_{ijk}+\sqrt{\rho_{i+1,j,k}}v_{i+1,j,k}}{\sqrt{\rho_{ijk}}+\sqrt{\rho_{i+1,j,k}}}\,;$$
$$\bar{w}_{i+1/2} = \frac{\sqrt{\rho_{ijk}}w_{ijk}+\sqrt{\rho_{i+1,j,k}}w_{i+1,j,k}}{\sqrt{\rho_{ijk}}+\sqrt{\rho_{i+1,j,k}}}\,; \quad \bar{c}_{i+1/2} = \begin{cases} \left(\frac{p_{i+1,j,k}-p_{i,j,k}}{\rho_{i+1,j,k}-\rho_{i,j,k}}\right)^{0.5}, & |\rho_{i+1,j,k}-\rho_{i,j,k}| > 10^{-12} \\ \frac{1}{\sqrt{\rho_{i,j,k}}}, & |\rho_{i+1,j,k}-\rho_{i,j,k}| \le 10^{-12} \end{cases};$$
$$\bar{\rho}_{i+1/2} = \sqrt{\rho_{i,j,k}\rho_{i+1,j,k}}. \tag{28}$$

We have omitted for brevity the superscript n by the components of the vector $\bar{\mathbf{U}}_{i+1/2}$ in formulas (28). The expressions for the entries of matrix $\bar{\bar{\mathbf{A}}}$ also contain the quantities $\hat{u} = \xi_x u + \xi_y v$, $\hat{v} = \eta_x u + \eta_y v$, and $\hat{w} = \zeta_x u + \zeta_y v + \zeta_z w$. Following [28] we computed the averages $\bar{\hat{u}}_{i+1/2}$,$\bar{\hat{v}}_{i+1/2}$,$\bar{\hat{w}}_{i+1/2}$ in matrix $\bar{\bar{\mathbf{A}}}$ by formulas:

$$\begin{aligned} &\bar{\hat{u}}_{i+1/2} = \xi_{x,i+1/2}\bar{u}_{i+1/2} + \xi_{y,i+1/2}\bar{v}_{i+1/2}; \quad \bar{\hat{v}}_{i+1/2} = \eta_{x,i+1/2}\bar{u}_{i+1/2} + \eta_{y,i+1/2}\bar{v}_{i+1/2}; \\ &\bar{\hat{w}}_{i+1/2} = \zeta_{x,i+1/2}\bar{u}_{i+1/2} + \zeta_{y,i+1/2}\bar{v}_{i+1/2} + \zeta_{z,i+1/2}\bar{w}_{i+1/2}\,. \end{aligned} \tag{29}$$

The quantities $\xi_{x,i+1/2}$, $\xi_{y,i+1/2}$ in (29) were computed as the arithmetic means:

$$\xi_{x,i+1/2} = (1/2)[(\xi_x)_{ijk} + (\xi_x)_{i+1,j,k}; \quad \xi_{y,i+1/2} = (1/2)[(\xi_y)_{ijk} + (\xi_y)_{i+1,j,k}]. \tag{30}$$

The expressions for the matrices $\mathbf{R}_\nu$, $\nu = 1, 2, 3$, were found by us with the aid of CAS *Mathematica*. We will present the corresponding procedure at the example of matrix $\hat{\mathbf{A}}$. We at first present the expressions for matrices $\mathbf{A}$, $\mathbf{B}$, and $\mathbf{C}$ entering formulas

$$\mathbf{A}(\mathbf{U}) = \frac{\partial \mathbf{F}(\mathbf{U})}{\partial \mathbf{U}}, \quad \mathbf{B}(\mathbf{U}) = \frac{\partial \mathbf{G}(\mathbf{U})}{\partial \mathbf{U}}, \quad \mathbf{C}(\mathbf{U}) = \frac{\partial \mathbf{H}(\mathbf{U})}{\partial \mathbf{U}}\,. \tag{31}$$

$$\mathbf{A} = \begin{pmatrix} 0 & 1 & 0 & 0 \\ c^2-u^2 & 2u & 0 & 0 \\ -uv & v & u & 0 \\ -uw & w & 0 & u \end{pmatrix}, \quad \mathbf{B} = \begin{pmatrix} 0 & 0 & 1 & 0 \\ -uv & v & u & 0 \\ c^2-v^2 & 0 & 2v & 0 \\ -vw & 0 & w & v \end{pmatrix}, \quad \mathbf{C} = \begin{pmatrix} 0 & 0 & 0 & 1 \\ -uw & w & 0 & u \\ -vw & 0 & w & v \\ c^2-w^2 & 0 & 0 & 2w \end{pmatrix}$$

In the expansion

$$\hat{\mathbf{A}} = J\,(\xi_x\mathbf{A} + \xi_y\mathbf{B}) = \mathbf{R}_1\mathbf{\Lambda}_1\mathbf{R}_1^{-1} \tag{32}$$

$\mathbf{\Lambda}_1$ is a diagonal matrix whose diagonal entries are the eigenvalues of matrix $\hat{\mathbf{A}}$, and the multiple eigenvalues are repeated on the diagonal in accordance with their multiplicity. Let $\mathbf{X}_k$ be the right eigenvector of matrix $\hat{\mathbf{A}}$, that is $\mathbf{X}_k$ satisfies the equation $\hat{\mathbf{A}}_k\mathbf{X}_k = \lambda_k\mathbf{X}_k$, $k = 1, ..., 4$. Then the columns of the matrix $\mathbf{R}_1$ in the expansion (32) are known to be composed of the coordinates of the right eigenvectors of matrix $\hat{\mathbf{A}}$, that is $\mathbf{R}_1 = (\mathbf{X}_1|\mathbf{X}_2|\mathbf{X}_3|\boldsymbol{X}_4)$. The vertical bars in this formula separate one column from another. Let similarly $\mathbf{Y}_k$ be the left eigenvector of matrix $\hat{\mathbf{A}}$, which corresponds to the eigenvalue λ_k, that is $\mathbf{Y}_k$ satisfies the equation $\mathbf{Y}_k\hat{\mathbf{A}} = \lambda_k\mathbf{Y}_k\,, \quad k = 1, ..., 4$. The lines of matrix $\mathbf{R}_1^{-1}$ in expansion (32) then consist of the coordinates of the left eigenvectors of matrix $\hat{\mathbf{A}}$, that is

$$\mathbf{R}_1^{-1} = \begin{pmatrix} \mathbf{Y}_1 \\ \hline \mathbf{Y}_2 \\ \hline \mathbf{Y}_3 \\ \hline \mathbf{Y}_4 \end{pmatrix},$$

where the horizontal bars separate one line from another.

For the computation of matrices $\mathbf{R}_1$ and $\mathbf{\Lambda}_1$ in the expansion of matrix $\hat{\mathbf{A}}$ (32) one can use the following built-in functions of the software system *Mathematica* 4.1, respectively: `Eigenvalues`[**A**] and `Transpose[Eigenvectors`[**A**]]. There is also the built-in function `JordanDecomposition`[**A**], which outputs simultaneously $\mathbf{R}_1$ and $\mathbf{\Lambda}_1$. Therefore, we have used this function in view of its convenience:

$$[\mathtt{R}_1, \mathit{\Lambda}_1]\mathtt{= JordanDecomposition[As]},$$

where $\mathtt{As} \equiv \quad \hat{\mathbf{A}}$, and

$$\mathit{\Lambda}_1 = \mathrm{diag}(\lambda_1^{(1)}, \lambda_2^{(1)}, \lambda_3^{(1)}, \lambda_4^{(1)}),\ \lambda_1^{(1)} = \lambda_2^{(1)} = J\hat{u}, \quad \lambda_3^{(1)} = \lambda_1^{(1)} - Jc|\nabla\xi|\,, \quad \lambda_4^{(1)} = \lambda_1^{(1)} + Jc|\nabla\xi|\,,$$

$$|\nabla\xi| = \sqrt{\xi_x^2 + \xi_y^2}, \quad \hat{u} = \xi_x u + \xi_y v.$$

As a result, the following expression for matrix $\tilde{\mathbf{R}}_1$ was found:

$$\tilde{\mathbf{R}}_1 = \begin{pmatrix} 0 & 0 & \frac{1}{w} & \frac{1}{w} \\ 0 & -\frac{\xi_y}{\xi_x} & \frac{-c\xi_x + u|\nabla\xi|}{w|\nabla\xi|} & \frac{c\xi_x + u|\nabla\xi|}{w|\nabla\xi|} \\ 0 & 1 & \frac{-c\xi_y + v|\nabla\xi|}{w|\nabla\xi|} & \frac{c\xi_y + v|\nabla\xi|}{w|\nabla\xi|} \\ 1 & 0 & 1 & 1 \end{pmatrix}. \tag{33}$$

While deriving formula (33) we have used the fact that the derivative $\xi_z = 0$ according to (10). This has resulted in a significant simplification of the expressions for the entries of matrix $\tilde{\mathbf{R}}_1$.

It can be seen from (33) that there is the velocity component w in the denominators of some entries. Thus, a singularity arises in these entries at $w = 0$. On the other hand it is well known that the matrix $\tilde{\mathbf{R}}_1$ in the Jordan decomposition is determined non-uniquely. Let indeed $\mathbf{D}_1$ be a nonsingular diagonal matrix, and let $\mathbf{R}_1 = \tilde{\mathbf{R}}_1\mathbf{D}_1$. Consider the expression for $\mathbf{R}_1\mathbf{\Lambda}_1\mathbf{R}_1^{-1}$:

$$\mathbf{R}_1\mathbf{\Lambda}_1\mathbf{R}_1^{-1} = \tilde{\mathbf{R}}_1\mathbf{D}_1\mathbf{\Lambda}_1\left(\tilde{\mathbf{R}}_1\mathbf{D}_1\right)^{-1} = \tilde{\mathbf{R}}_1\mathbf{D}_1\mathbf{\Lambda}_1\mathbf{D}_1^{-1}\tilde{\mathbf{R}}_1^{-1} = \tilde{\mathbf{R}}_1\mathbf{\Lambda}_1\tilde{\mathbf{R}}_1^{-1} = \hat{\mathbf{A}}.$$

Thus, we can try to choose such a diagonal matrix $\mathbf{D}_1$, which eliminates the singularity in the entries of matrix (33). This requirement is met by the following matrix $\mathbf{D}_1$: $\mathbf{D}_1 = \mathrm{diag}(c, c\xi_x, w, w)$. As a result we obtain:

$$\mathbf{R}_1 = \tilde{\mathbf{R}}_1\mathbf{D}_1 = \begin{pmatrix} 0 & 0 & 1 & 1 \\ 0 & -c\xi_y & -c\hat{\xi}_x + u & c\hat{\xi}_x + u \\ 0 & c\xi_x & -c\hat{\xi}_y + v & c\hat{\xi}_y + v \\ c & 0 & w & w \end{pmatrix},\ \mathbf{R}_1^{-1} = \begin{pmatrix} -\frac{w}{c} & 0 & 0 & \frac{1}{c} \\ \frac{u\xi_y - v\xi_x}{c|\nabla\xi|^2} & \frac{-\xi_y}{c|\nabla\xi|^2} & \frac{\xi_x}{c|\nabla\xi|^2} & 0 \\ \frac{1}{2}\left(1 + \frac{\hat{\xi}_x u + \hat{\xi}_y v}{c}\right) & -\frac{\hat{\xi}_x}{2c} & -\frac{\hat{\xi}_y}{2c} & 0 \\ \frac{1}{2}\left(1 - \frac{\hat{\xi}_x u + \hat{\xi}_y v}{c}\right) & \frac{\hat{\xi}_x}{2c} & \frac{\hat{\xi}_y}{2c} & 0 \end{pmatrix}, \tag{34}$$

where $\hat{\xi}_x = \xi_x/|\nabla\xi|,\ \hat{\xi}_y = \xi_y/|\nabla\xi|$. Note that $\mathrm{Det}(\mathbf{R}_1) = -2c^3|\nabla\xi| < 0$, thus, the matrix $\mathbf{R}_1$ is nonsingular. The expressions for the matrices $\mathbf{R}_2$, $\mathbf{R}_2^{-1}$, $\mathbf{R}_3$, $\mathbf{R}_3^{-1}$ were found in a similar way with the aid of CAS *Mathematica* and are not presented here for the purpose of brevity.

It is to be noted that the Roe's fluxes (23), (24), and (25) also involve the products $\mathbf{R}_\nu\psi(\mathit{\Lambda}_\nu)\mathbf{R}_\nu^{-1}$, $\nu = 1, 2, 3$. The computation of these products by hand would be a very tedious and error prone task, so that we have computed them with *Mathematica*. The expressions for the entries of matrices $\mathbf{R}_\nu\psi(\mathit{\Lambda}_\nu)\mathbf{R}_\nu^{-1}$ were exported from *Mathematica* to a file in Fortran form. These ready Fortran lines were then inserted into three subroutines for the computation of the Roe's fluxes.

6 Numerical results

The results of numerical computations presented in Fig. 4 were obtained for the case of a discontinuous pressure function at the lower compensator inlet, which were periodic in time with the frequency of pressure oscillations $f = 25$ Hz. The mean pressure in the outlet compensator section was computed as the arithmetic mean of the pressure values at cell centers in this section. The pictures of the local fluid velocity vectors inside the compensator obtained for different moments of time show that the shock wave propagating upwards in the compensator pushes the liquid upwards in the direction opposite to the direction of liquid pumping in the PRDH (see Fig. 4, a).

An analysis of the pictures of pressure and density contours in different sections along the longitudinal axis of the spiral channel has not revealed any phenomena of the reflection or diffraction

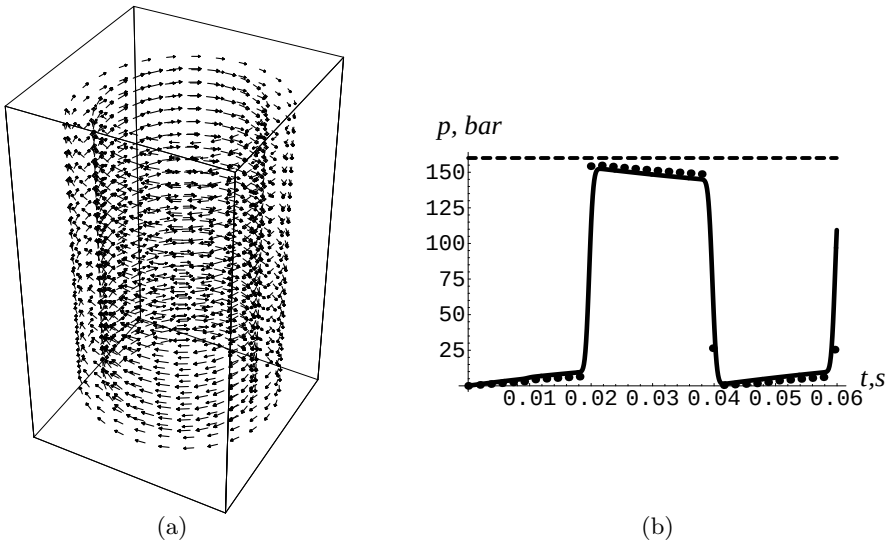

(a) (b)

Fig. 4. The results of a three-dimensional computation of fluid flow in a spiral compensator at $t = 0.05996$ sec.: (a) the vector field plot; (b) the mean pressure value as a function of time at the outlet section of the compensator; the dotted line is the result of one-dimensional computation by a TVD scheme from [22].

of shock waves. This is related, in particular, to the fact that the walls of the spiral channel under consideration have a constant curvature along any of the ξ, η or ζ directions.

The results of three-dimensional numerical computations carried out for the cases of a discontinuous and smooth boundary condition for the pressure at the lower inlet of the compensator show that at the consideration of the three-dimensional flow character the effect of the damping of shock waves during their motion upwards in the compensator proves to be somewhat stronger than in the computations based on the one-dimensional model (see Fig. 4, b). It has been shown that for a further enhancement of the damping of shock waves in the compensator it is desirable to ensure an additional smoothing of the discontinuous pressure profile at the lower inlet of the compensator. This may be achieved by mounting an additional valve supported by a spring, whose strength must be adjusted.

Conclusion

We have shown above how the computer algebra systems can be used at various stages of both the formulation of the mathematical model describing a complex fluid flow process and the derivation of the formulas necessary to implement a specific finite-difference method on a curvilinear spatial grid. Our estimates show that we have saved at least one month of work of one person in comparison with the case of the implementation of all stages of mathematical modelling and computer code writing by hand.

References

1. Akers, R.L., Kant, E., Randall, C.J., Steinberg, S. and Young, R.L.: SciNapse: A problem-solving environment for partial differential equations. *IEEE Computational Science an Engineering* **4** (1997), No. 3, 32–42
2. Blaschke, W.: *Einführung in die Differentialgeometrie.* Springer, Berlin, Heidelberg (1950)
3. Blazek, J.: *Computational Fluid Dynamics: Principles and Applications.* Elsevier, Amsterdam, London, New York (2001)
4. Engelen, van R.: Ctadel: A generator of Efficient Codes. Ph.D. Thesis, LIACS, Leiden University (1998)
5. Ferziger, J.H., Perić, M.: *Computational Methods for Fluid Dynamics*, 3rd Edition, Springer-Verlag, Berlin, Heidelberg (2002)

6. Ganzha, V.G., Chibisov, D., Vorozhtsov, E.V.: GROOME – tool supported graphical object oriented modelling for computer algebra and scientific computing. In: *Computer Algebra in Scientific Computing/ CASC 2001*, V.G. Ganzha, E.W. Mayr, E.V. Vorozhtsov (Eds.), Springer-Verlag, Berlin (2001) 213–232
7. Ganzha, V., Chibisov, D., Vorozhtsov, E.: Problem solving for scientific computing: data modelling instead of algorithms? *Selçuk J. Appl. Math.* **12** (2001) 53–72
8. Ganzha, V.G., Chibisov, D., Vorozhtsov, E.V.: Computer algebra in problem solving for computational flui dynamics: term rewriting and all that. In: *Computer Algebra in Scientific Computing/ CASC 2002*, V.G. Ganzha, E.W. Mayr, E.V. Vorozhtsov (Eds.), Technical University of Munich, Munich (2002) 85–96
9. Ganzha, V.G., Chibisov, D., Vorozhtsov, E.V.: Object oriented modelling in numerical computations: multigrid calculations using Maple. In: *Computer Algebra in Scientific Computing/ CASC 2003*, V.G. Ganzha, E.W. Mayr, E.V. Vorozhtsov (Eds.), Technical University of Munich, Munich (2003) 121–141
10. Ganzha, V.G., Shashkov, M.Yu., Solovyov, A.V.: Algorithms for operations with difference operators and grid functions in symbolic form. In: *Computer Algebra and Its Applications to Mechanics, CAAM'90. Proc. Int. Seminar, Novosibirsk, August 28–31, 1990; Irkutsk, September 1–3, 1990*, V.G. Ganzha, V.M. Rudenko and E.V. Vorozhtsov (Eds.), Nova Science Publishers, Inc., New York, (1993) 63–69
11. Ganzha, V., Vorozhtsov, E.: Diagram design and analysis of aerodynaamics problems with Mathematica, *Selçuk J. Appl. Math.* **1** (2000) 21–46
12. Heitlager, I., Engelen, van R., Wolters, L.: *The Construction of Flux-Limiting Advection Algorithms through Program Generation*, Technical report No. 98-04, University of Leiden, Leiden, The netherlands (1998) 1–25
13. Hutarew, G.: *Einfürung in die Technische Hydraulik*. Springer-Verlag, Berlin, Göttingen, Heidelberg (1965)
14. Jenkner, W.R.: Über die Druckstossgeschwindigkeit in Rohrleitungen mit quadratischen und rechteckigen Querschnitten. Schweizerische Bauzeitung. Heft 5 (1971) 99–103
15. Kiselev, S.P., Vorozhtsov, E.V., Fomin, V.M.: *Foundations of Fluid Mechanics with Applications: Problem Solving Using Mathematica*. Birkhäuser, Boston, Basel, Berlin (1999)
16. Knupp, P., Steinberg, S.: *Fundamentals of Grid Generation*. CRC Press, Boca Raton, Ann Arbor (1994)
17. Liska, R., Drska, L.: FIDE: A REDUCE package for automation of FInite difference method for solving pDE. In: *Proc. Int. Symp. on Symbolic and Algebraic Computation, ISSAC'90, August 20–24, 1990, Tokyo, Japan*, S. Watanabe and M. Nagata (Eds.), ACM Press, New York (1990) 169–176
18. Liska, R., Shashkov, M.Yu.: Algorithms for difference scheme construction on non-orthogonal logically rectangular meshes. In: *Proc. 1991 Int. Symp. on Symbolic and Algebraic Computation, ISSAC'91, July 15–17, 1991, Bonn, Germany*, S.M. Watt (Ed.), ACM Press, New York (1991) 419–426
19. MACSYMA Reference Manual (version 13), Symbolics, Inc. (1988)
20. Mark, P. van der, Wolters, L., Cats, G.: Automatic code generation for a convection scheme. In: *proc. 18th ACM Sympos. on Applied Computing, March 2003, Melbourne (Fl., USA)*, ACM Press, New York (2003) 1003–1008
21. Pixton, D.S.: *A New Generation Mud Driven Rotary Percussion Tool*. Novatek, Provo, Utah (1990)
22. Schacht, W., Vorozhtsov, E.V., Voevodin, A.F., Ostapenko, V.V.: Numerical modelling of hydraulic jumps in a spiral channel with rectangular cross section. *Fluid Dynamics Research* **31** (2002) 185–213
23. Steinberg, S., Roache, P.: Finite-difference algorithm design and automatic code generation. In: *Computer Algebra and Its Applications to Mechanics, CAAM'90. Proc. Int. Seminar, Novosibirsk, August 28–31, 1990; Irkutsk, September 1–3, 1990,* V.G. Ganzha, V.M. Rudenko and E.V. Vorozhtsov (Eds.), Nova Science Publishers, Inc., New York, (1993) 15–29
24. Swaffield, J.A., Boldy, A.P.: *Pressure Surge in Pipe and Duct Systems*. Avebury Technical, Aldershot, Brookfield, USA, Hong Kong, Singapore, Sydney (1993)
25. Toro, E.F.: *Riemann Solvers and Numerical Methods for Fluid Dynamics. A Practical Introduction*, Springer-Verlag, Berlin, New York (1999)
26. Voevodin, A.F., Shugrin, S.M.: *Numerical Methods for Calculating One-Dimensional Systems*. Nauka, Siberian Branch, Novosibirsk (in Russian) (1981)
27. Vysotina, V.G.: Modelling of inviscid gas flow in axisymmetri channels with the flow turn by 180 and 540 degrees. *Matemticheskoe Modelirovanie* **8**, No. 10 (1996) 25–34
28. Yamamoto, S., Daiguji, H.: Higher-order-accurate upwind schemes for solving the compressible Euler and Navier–Stokes equations. *Computers and Fluids* **22** (1993) 259 – 270
29. Zhao, G.: *Entwicklung und Optimierung eines hydraulischen Bohrhammers*. Mitteilungen aus dem Institut für Erdöl- und Erdgastechnik der Technischen Universität Clausthal, Clausthal – Zellerfeld (1998)